Hybrid Ant Colony Optimization–Convolutional Neural Network Framework for Intelligent Performance Enhancement and Fault Diagnosis in DFIG Wind Turbines

SubhaSeethalakshmi V[1*], Praveen B. M[2], Vengadachalam N[3], Balakrishnan P[4]

[1*]Post-Doctoral Fellow, Institute of Engineering and Technology, Srinivas University, Mukka, Surathkal, Mangaluru, Karnataka, India, +91 9047015816,

[2]Director, Research and Innovation Council of Srinivas University, Mukka, Surathkal, Mangaluru, Karnataka, India, +919980951074,

[3]Associate Professor, Department of Electrical Engineering, AnnasahebDange College of Engineering &Technology, Ashta, Sangli, Maharashtra, India, +919944950505,

[4]Associate Professor, Department of Electrical & Electronics Engineering, J. J College of Engineering & Technology, Ammapettai, Tiruchirappalli, Tamilnadu, India, +91 944274327,

Abstract

A hybrid Ant Colony Optimization-Convolutional Neural Network (ACO-CNN) was designed as a way of enhancing performance monitoring and fault diagnostics of Doubly-Fed Induction Generator (DFIG) wind turbines. It was done by simulating the operation of DFIG in normal and faulty conditions. The simulations produced electrical, mechanical signals, including stator currents, rotor currents, speed, torque, and power. Preprocessing parameter optimization was done with Ant Colony Optimization (ACO). It optimized the selection of features, filters, and windows of segmentation. This was done in order to ensure that only good quality and noise reduced signals were made available to train on. A specialized Convolutional Neural Network CNN model was utilized using the optimized signals. The CNN learnt hierarchical features and discriminated normal and defective states of operation. The framework was experimented and was discovered that the ACO-CNN was accurate compared to a conventional CNN. It achieved a score of approximately 96.8% and 89.6% with raw CNN input respectively. The recall, precision and training convergence speed was improved. In a variety of fault conditions, such as converter faults, rotor anomalies and grid voltage dips, classification was found to have an average of 95.8%.

Keywords - Ant Colony Optimization, Doubly-Fed Induction Generator, Convolutional Neural Network, Fault Diagnosis, Condition Monitoring

1 Introduction

DFIG wind turbines are still predominant onshore, especially in their fleets. Where converters on the rotor side consume a fraction of the rated power. This enables the variable-speed operation at affordable cost in contrast to full-scale converters [1]. Currently, more developed studies are directed at adherence to the new grid codes, where reactive power support, the low-voltage ride-through (LVRT) and weak grid stability are currently discussed as the main aspects [2]. New controllers are directed at greater robustness and quicker transience reaction. Similar experiments were conducted on aero-electrical co-simulation and condition monitoring. Cuts of downtime and life-cycle costs were made with the help of SCADA and vibration data [3]. The level of advancements is concentrated in the area of LVRT enhancement, solid control and optimization. Fractional-order, sliding-mode, and model-predictive designs were experimented and they were discovered to enhance rejectance of disturbances and the control of voltages and currents [4]. Commissioning Metaheuristic PI tuning, fuzzy and fractional-order controllers accelerated commissioning and assisted in raising the margins of dynamic stability. LVRT plans have grid-side and rotor-side converters coordinated [5]. DC-link limits and reactive power were adjusted to achieve a higher level of codes to enhance the weak-grid operations. It has also been observed that MPPT improves in turbulence. Wind and PV hybrids were determined to be useful in terms of grid support coordination [6]. Three levels of performance were enhanced, maximising energy capture, stabilising will be generator-converter dynamics and enhancing grid support. PI and fuzzy controllers were optimized in order to achieve lower overshoot and torque ripple. Excursions of DC-link were kept low during faults and gusts [7]. PLL strategies and reactive power are useful in enhancing weak grids stability. Swarm and genetic directed MPPT improve tip-speed ratio tracking. Such gains are confirmed by advanced tests. Metaheuristic optimized controllers provide higher settling and reduced THD, but do not compromise steady-state efficiency [8].

DFIG drives also experience electrical problems including IGBT failures and imbalances and mechanical failures of bearings and gearboxes. The issues decrease the quality of power and jeopardize LVRT compliance. This has to be detected early to avoid cascading trips which can lower the maintenance cost and conserve the availability of the turbines [9]. Incipient gearbox defects are missed by the traditional spectral methods. New multimodal sensing and analytics are used to process electrical and vibration signals by learning based classifiers. There has been an improvement in detections and fault isolation. Condition-based maintenance is more effective when using transient features of DFIG specific and deep models. Clustering in the internet was observed to be quicker and more powerful [11]. Optimization is seen in the design, control and operation levels, which inform the ratings and the selection of filters. It assists in adjusting gains and current limits. Particle swarm, genetic algorithms, bacterial foraging, and ant colony, are the metaheuristics that prevail over the other traditional methods. These techniques co-tune the controllers of RSC, GSC systems and pitch systems [12]. Multi-objective criterion are the settling time, overshoot, harmonic distortion and reactive support with hybrid algorithms exhibiting better convergence. LVRT coordination was done to minimize stress on converter limits, DC-link choppers and reactive power priorities. Benchmarks ensure steady dynamic performance and increase in energy yields [13].

The ant colony optimization (ACO) is implemented when we do not have the gradient or where the models are not nonconvex. It has been used in fractional-order controllers and integral sliding-mode. It is also applied in tuning PLL parameters, RSC torque loops and MPPT in the presence of turbulence. ACO achieves a balance between exploration and exploitation based on pheromone updates. It controls aggregate LVRT limitations, converter limits and reactive power demands. It reduces DC-link ripple, ITAE and THD. Research indicates that ACO is equivalent to GA and PSO. It is resistant to noise and parameter drifts [14]. Multimodal and learning-based diagnostics Multimodal diagnostics (EMSCADA fused) is used in condition monitoring. This identifies failure in gearboxes, bearings and converters. The classical ANNs are still significant in life prediction and classification. Anomaly detection based on unsupervised techniques requires fewer labels. More recent deep hybrid models including CNN-LSTM and attention-based are used to capture both spatial and temporal characteristics in signals [15]. Through this, the level of accuracy in the detection of multiple faults is enhanced significantly. According to case studies, there are advantages when electrical data is combined with vibration data. ANN classifiers identify early IGBT open-circuit faults and machine learning minimizes false trips and improves the LVRT and reduces downtime [16]. Convolutional neural networks (CNNs) are fed information that are in the form of raw or pre-processed signals. Vibrations, current and voltage are inputs, transformed into spectrograms and scalograms, and classified by 2D-CNNs, which are better than hand-crafted feature approaches. In 1D-CNNs and CNN-LSTM hybrids, 1D-CNNs are applied in temporal dynamics [17]. These enhance resistance to changes in operating point. The literature about DFIG turbines is still improving on control, optimization, and machine learning. Individual works presented metaheuristic tuning and diagnostics of deep learning. Nevertheless, there are still limited integrated frameworks. This study hypothesizes an integrated ACO-CNN system to optimize the work of turbines and fault detection.

2. Materials & Methods

2.1 Doubly-Fed Induction Generator Wind turbine

The Doubly-Fed Induction Generator (DFIG) that was discussed in this study was a wound-rotor induction machine with the stator windings hard-wired to the grid and with the rotor windings hard-wired to a back-to-back power electronic converter. With this arrangement, the active and reactive power could be independently controlled, which makes the DFIG appropriate to comply with grid codes and fault ride-through. DFIG system has been modeled in three major sections. Power is passed directly to the grid by the stator circuit. Slip rings were used to connect the rotor circuit to the rotor side converter (RSC). A DC-link capacitor was used to connect the grid-side converter (GSC) to the grid. RSC controlled rotor currents to obtain torque and flux control which made possible to track maximum power point with variable wind speed. Meanwhile, the GSC was able to sustain DC-link voltage stability, as well as to control the reactive power exchange with the grid [18]. To run a simulation and collect data, a DFIG model has applied flux linkages, stator and rotor voltage equations and Park transformation to a d-q axis analysis. The operational conditions were normal generation, unbalanced grid fault, voltage dips, and rotor-related abnormalities [19]. Such simulations generate mechanical and electrical signals that include rotor speed oscillations, currents, power and rotor speed, which was utilized in augmentation of performance and fault grouping investigations. Figure 1 is the schematic diagram of the DFIG.

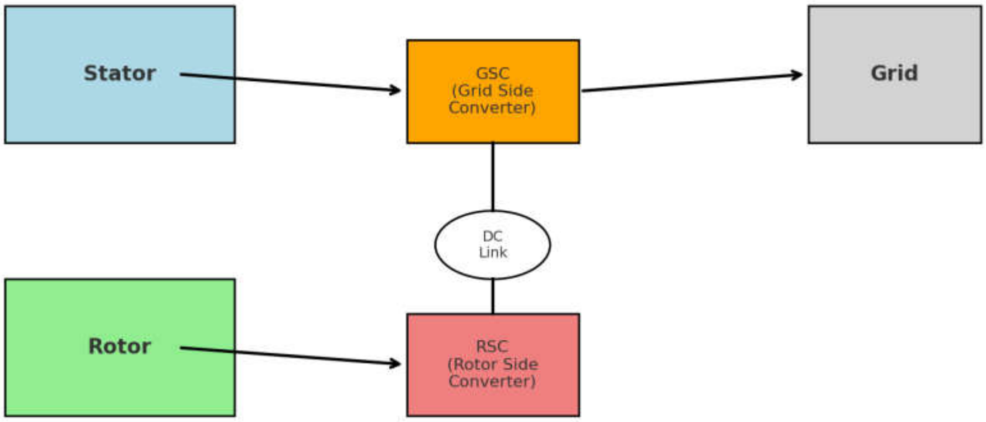

Figure 1. Schematic representation of DFIG

2.2 Data collection

Within the suggested structure, the control of a Doubly-Fed Induction Generator (DFIG) wind turbine was based on the thorough information gathering of mechanical subsystem and electrical subsystem. The signals were well chosen to record the normal operation behavior and to highlight the abnormalities that occur due to converter, electrical or mechanical defects. These indicators formed the foundation of control optimization, condition monitoring as well as the fault classification framework. These electric signals are stator voltages, stator currents, rotor currents, DC-link voltage, reactive and active power. Stator currents (Ia, Ib, Ic) played a key role in identifying unbalanced conditions, converter fault and harmonics since the abnormal signatures indicated faults of the winding and grid. Stator voltages were also important indications of grid-side disturbances including asymmetries, sags and swells which directly affect the performance of the generators. Rotor currents were also essential in detecting problems with the converters like broken rotor bars and open circuits gathered through slip rings. Monitor of the DC-link voltage was used to record the variations that are indicative of power electronic instability, converter malfunctions and over torque vibrations. Active and reactive power P, Q was also monitored, because changes in these two quantities are indications of unbalanced operating conditions, aerodynamic anomalies and grid-related problems, and correct reactive power regulation will maintain voltage support to the grid. Signals like electromagnetic torque, rotor speed, vibrations and acoustics were taken into account on the mechanical side. The rotor speed was necessary in monitoring slip and maximum power point tracking besides speed oscillations to point out gearbox defects or other mechanical load disturbance. Electromagnetic torque is calculated using the electric equations and indicated when there was an oscillation, which is indicative of a misalignment of the shafts, and electrical faults. Vibration and acoustic analysis were used to help identify degradation of bearings, wear of the gear box and other structural imbalances [20].

Negative-sequence components and total harmonic distortion (THD) were used to assess the quality of power. High values of THD in stator voltages and currents indicated converter switching issues/resonance conditions but the negative-sequence components were an indication of unbalanced grid that subjected the machine to mechanical and thermal load. Besides, environmental and operational parameters, including wind speed and pitch angle were observed. The wind speed, recorded at nacelle mount sensors and were required to match the output of turbines to aerodynamic input. The pitch angle was also observed as one of the parameters to evaluate the effectiveness of aerodynamic control, especially during fault ride-through work, and it guaranteed the stability and the productivity of the given turbine functioning. Table 1 displays the normal operation DFIG signals.

Table 1 Operating Signal Ranges of the DFIG Wind Turbine Monitoring

Signal	Normal Value Range	Remarks
Stator Currents (Ia, Ib, Ic)	0.9–1.1 pu	Balanced sinusoidal currents
Stator Voltages	0.98–1.02 pu	Stable, symmetrical, grid-connected
Rotor Currents	0.1–0.25 pu	Smooth, within control limits
DC-Link Voltage	1050–1150 V	Ripple < 5%
Active Power (P)	0.5–2 MW (based on wind)	Stable output proportional to wind speed
Reactive Power (Q)	-0.2 to +0.2 pu	Within limits, supports grid voltage
Rotor Speed	1000–1500 rpm	Variable-speed tracking wind input
Electromagnetic Torque	6–12 kNm	Smooth, oscillations < 5%
THD (Current/Voltage)	<5%	Clean power quality
Negative-Sequence Component	<2%	Minimal grid unbalance
Wind Speed	5–12 m/s (typical operation)	Correlates with stable power output
Pitch Angle	2°–15°	Adjusted for aerodynamic control

Table 1 showed the normal operating values of major mechanical, electrical and environmental signals of a DFIG wind turbine. Stator currents were held in balance at 0.9-1.1 pu and the stator voltages were maintained at 0.98-1.02pu, to allow adequate connection to the grid. Smooth converter operation was observed in the 0.1-0.25 pu rotor currents. DC-link voltage during operation was kept at higher than lower limits of 1050 and within upper limits of 1150 V and at less than 5 percent ripple. Active power was 0.5-2 MW with wind speed whereas reactive power was -0.2 to +0.2 pu with grid voltage. Rotor speed was followed to wind input of 1000-1500 rpm and electromagnetic torque was held between 6-12 kNm and oscillation was kept at minimal range. The quality of power was checked with THD less than 5 percent and a negative-sequence less than 2 percent. The environmental signal was the wind speed of 5-12 m/s and the adjustments of the pitch angle was 2deg-15deg which guaranteed the aerodynamic efficiency and stability in the power generation. Table 2 displays the fault values of the key signals of a DFIG wind turbine.

Table 2 Fault Signal Ranges for DFIG Wind Turbine

Signal	Fault Value Range	Fault Indication
Stator Currents (Ia, Ib, Ic)	>1.4 pu or unbalanced (>10%)	Winding fault, grid asymmetry, short-circuit
Stator Voltages	<0.9 pu (sag) or >1.1 pu (swell)	Grid disturbance, poor ride-through
Rotor Currents	>0.4 pu with harmonics	Rotor anomaly, converter switching fault
DC-Link Voltage	<900 V or >1200 V ripple >10%	Converter instability, IGBT fault
Active Power (P)	Sudden drop or oscillation ±20%	Aerodynamic mismatch, shaft defect, grid trip
Reactive Power (Q)	Beyond ±0.4 pu	Poor reactive support, GSC malfunction
Rotor Speed	Oscillations > ±15% nominal	Gearbox fault, shaft misalignment
Electromagnetic Torque	Oscillations >20%	Converter fault, unbalanced magnetic pull
THD (Current/Voltage)	>8%	Converter malfunction, harmonic resonance
Negative-Sequence Component	>5%	Grid unbalance, stator winding fault
Wind Speed	>20 m/s or <3 m/s	Operating beyond cut-in/cut-out limit
Pitch Angle	Not adjusting properly (0° or >30° fixed)	Pitch actuator failure, aerodynamic control fault

Table 2 detailed the scope of fault values of vital signals in a DFIG wind turbine and the potential hints. During grid asymmetry, winding faults and short circuits, stator currents are over 1.4 pu, or unbalanced above 10%. Under the circumstances of poor ride-through capability or when the power grid suffers disturbances the voltage levels might even drop below 0.9 per unit (pu) or even rise to beyond 1.1 per unit (pu); this is an unstable or abnormal operating condition in the electrical system. Converter switching faults and rotor anomalies caused the rotor current to rise above 0.4 pu and the harmonics respectively. In converter instability the DC-link voltage varied in excess, and reached values lower than 900 V or higher than 1200 V, with serious voltage ripple. Active power experiences sudden drops, or +20 percent swings, which are caused by aerodynamic discontinuities and shaft problems. GSC become ill at reactive power above +-

0.4 pu. High amplitudes of rotor speed oscillation and torque variation are signs of misalignments, gearbox, and converter defects. The presence of high THD, negative sequence components, abnormal wind speed, or set wind angle pitch indicates grid imbalance, converter issues and aerodynamic control failures [21].

2.3 Ant Colony Optimization (ACO)

The Ant Colony Optimization (ACO) metaheuristic tool was proposed. It was simulated after the foraging behavior of real ants. During the search of food, ants leave pheromones. The shorter routes accumulate greater amounts of pheromones with time. An even greater number of ants will be attracted by these paths and the best one will arise. This concept of group intelligence was reconfigured to resolve signal preprocessing in DFIG monitoring. Filter settings were tuned in this with the help of ACO. It picked the most pertinent features and partition the segment indicators in productive time windows. This eliminated noise and redundancy and only informative and clean signals were sent to the CNN classifier. The algorithm of the ACO was written mathematically. The first element was pheromone update rule where the possible paths were given a pheromone value. This was continually updated with an iteration. Solutions with stronger intensity were reinforced more and weaker ones lost the pheromone weight in time. Therefore, the algorithm approaches the best preprocessing strategy [22].

$T_{ij}(t+1) = (1-\rho).T_{ij}(t) + \Delta T_{ij}(t)$ ------------ Eq 1

In the above equation, $T_{ij}(t)$ is the pheromone level on edge (i,j) at iteration *t*, ρ∈(0,1) is pheromone evaporation rate (prevents unlimited accumulation) and $T_{ij}(t)$ are pheromone deposited by ants after constructing solutions. Next is Pheromone Deposit and for each ant *k* that selects path (i,j), the equation is

The above equation is defined as Tij (t) 0 = pheromone on edge (i,j) at iteration t, r? = pheromone evaporation rate (unlimited accumulation would otherwise occur), and Tij (t) = pheromone deposited by ants following the completion of solutions. Then, there is Pheromone Deposit and the equation is as follows:

$\Delta T_{ij}^{k} = \frac{Q}{L_k}$-----------------Eq 2

In the above equation, Q is the pheromone strength constant and L_k is the quality of the solution. The next equation is the Probability of Choosing a Path, wherein an ant choosing feature *j* with probability:

The pheromone strength constant in the above equation is Q and L k is the solution quality. The Probability of Choosing a Path is the next equation and is: an ant selecting feature j with probability:

$P_{ij}^{k}(t) = \frac{[T_{ij}(t)]^{\alpha}.[\eta_{ij}]^{\beta}}{\sum_{l\in N_i}[T_{il}(t)]^{\alpha}.[\eta_{il}]^{\beta}}$------------Eq 3

In the above equation, $\eta_{ij} = \frac{1}{L_{ij}}$ is the heuristic desirability (inverse of path cost, e.g., noise level) and α,β are parameters controlling influence of pheromone vs. heuristic. With repeated cycles, ACO will converge to a good preprocessing set that maximizes feature content to train CNN and therefore enhance classification efficiency in DFIG fault detection.

2.4 CNN and Hybrid ACO–CNN Framework

Convolutional Neural Network (CNN) was proposed as a deep learning model. It also automatically derives spatial and temporal characteristics in input data. In this study, CNN was trained to predict normal and abnormal conditions of a DFIG wind turbine. Training was then done by optimization of the input signals. CNN, unlike the traditional machine learning models, does not rely on feature extraction that has to be done manually. It picks up features on the basis of data. These characteristics were hierarchically organized. The simpler patterns were developed into lower layers and complex fault-related structures were developed in higher levels [23]. This automatic learning process will enhance detection of faults. CNN has three main layers:

The former is the Convolution Layer whereby filters (kernels) are used to identify local features. The equation is:

$$y_{i,j}^{(k)} = f\left(\sum_{m,n} x_{i+m,j+n} \cdot w_{m.n}^{(k)} + b^{(k)}\right) \text{-------------Eq 4}$$

In the above equation, x is input signal segment, $w^{(k)}$ are kernel weights, $b^{(k)}$ is bias and f is activation function.

Second is pooling layer and it diminishes dimensionality and still maintains important features. The one that is most predominant in a local area is picked by max-pooling. The equation can be expressed as follows

$$p_{i,j} = max(x_{i+m,j+n}) \text{ ----------------- Eq 5}$$

Third is totally linked layer. It uses combination of extracted features in order to make final classification (normal/fault). The equation can be expressed as follows:

$$z = f(W \cdot h + b) \text{ ---------Eq 6}$$

In the equation above, h represents the flattened feature, W represents the weights and b is bias. In case of Hybrid ACO-CNN Integration, the Ant Colony Optimization (ACO) was implemented as preprocessing optimizer, prior to CNN training. It optimized signal filtering levels. It stipulated the most relevant subsets of features. It divided the signals into good time windows. This was done to assure that the CNN only got high quality features. Noise was minimized and accuracy in classification was increased. During the optimization of the ACO, the fitness function was used. It tested the quality of each solution and changed pheromone levels respectively. The form of the fitness function is as follows:

$$F = \alpha \cdot Acc - \beta \cdot Err \text{ -------------Eq 7}$$

Acc in the above equation denotes CNN classification accuracy, Err denotes misclassification rate, and a,b are weighting factors. The hybrid ACO-CNN model was optimized successively until the best preprocessing settings were discovered. This combination takes advantage of the global search capability of ACO and the feature learning capability of CNN, which allows the intelligent performance improvement and fault diagnosis of the DFIG wind turbines. Figure 2 represents the schematic representation of ACO-CNN framework.

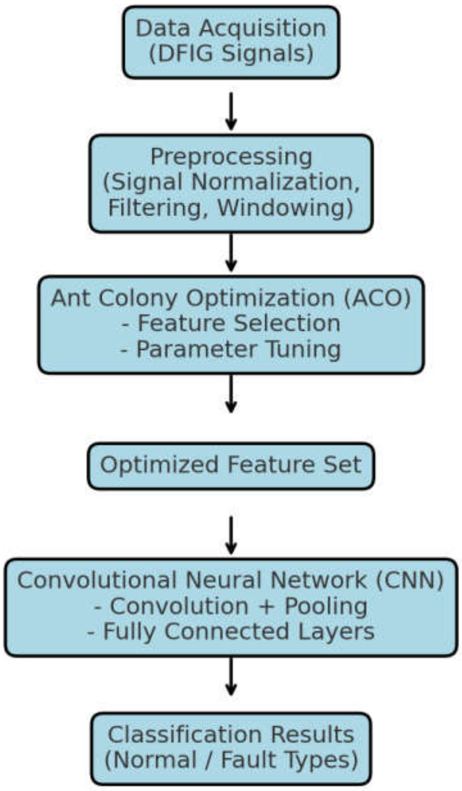

Figure 2 Schematic representation of ACO-CNN framework

3 Results & Discussions

The proposed Hybrid ACO-CNN model was run on the simulated data of the DFIG wind turbine. There were the normal and faulty conditions in the datasets. The framework combined preprocessing based on ACO and classification based on CNN. This integration not only improved the performance assessment, but it also resulted in a high degree of accuracy in fault diagnosis. The model has been seen to be strong in the management of various operating situations.

3.1 Performance Enhancement

The proposed Hybrid ACO-CNN framework was evaluated as compared to a baseline CNN, which was trained on raw data. This analogy illuminated obvious information on the position of optimization in fault diagnosis of DFIG wind turbines and ACO-based preprocessing stage took a center stage, to enhance signal quality and features representation. ACO gets the best filtering thresholds and select meaningful subsets of features. These measures eliminated unnecessary and noisy information. The absence of this process would cause the training process to slow down and generalization to become weak. This kind of refining was done selectively to guarantee that the CNN will be fed with a clean input space. The input was abundant in information and CNN was recovered discriminative patterns in a more reliable manner. Contrarily, CNNs that were trained on the raw features did not work well. Diagnostic accuracy was decreased in the presence of noise and irrelevant attributes. Also fault differentiations were weakened. ACO preprocessing was also found to enhance convergence in the training process as well as CNN required fewer epochs to stabilize, which saves calculation power. This efficiency was needed in the real time monitoring of wind turbines, which reduced false detection rate. The comparison outcomes are presented in Table 3.

Table 3. Performance Comparison (Raw CNN vs. ACO–CNN)

Model	Accuracy (%)	Precision (%)	Recall (%)	F1-Score (%)
CNN (Raw Data)	89.6	87.4	86.9	87.1
ACO–CNN (Optimized)	96.8	95.9	96.4	96.1

Table 3 validates the high effect of ACO optimization on CNN-based fault classification. The CNN which had been trained using the raw data attained a 89.6 per cent accuracy. Its accuracy, recall and the F1-scores were approximately 87%. These values demonstrate the adverse impact of noise as well as irrelevant features on learning models. With the introduction of ACO preprocessing, the optimised CNN fared a lot better, its accuracy rose to 96.8 and its precision came up to 95.9. This implied that false positives decreased. Recall increases to 96.4% and this is more sensitive to actual faults. F1-score was 96.1 which was equal performance on the evaluation measures. The precision increased by approximately 7.2 percent and the increase underscores greater strength. It also affirmed increased reliability of fault detection and greater computational efficiency [24].

3.2 Fault Diagnosis Results

Normal operating data was categorized 98% correctly. This mattered, because appropriate identification of healthy states will eliminate unnecessary alarms, as well as avoid expensive instances of interruption. In the case of faults, converters faults had 96.5 percent accuracy and rotor anomalies were 95.7 percent accurate. Stator unbalance was obtained to 94.9% and grid voltage dips were obtained to 93.8%. This reduced value is due to the fact that grid dips have some similarity with stator faults. This coincidence was identical to the trends in Figure 3 (Confusion Matrix). The figure had appropriate classification in the majority of cases. It also brought out slight misclassification between grid dip and stator fault. The confusion matrix gave a more detailed analysis of the performance of the classification. It juxtaposed the forecasted fault classifications with the real categories. It pointed out the merits of the hybrid framework in separating between normal and faulty states. The high diagonal figures identified the presence of accuracy and the few off-diagonal figures decreased misclassifications.

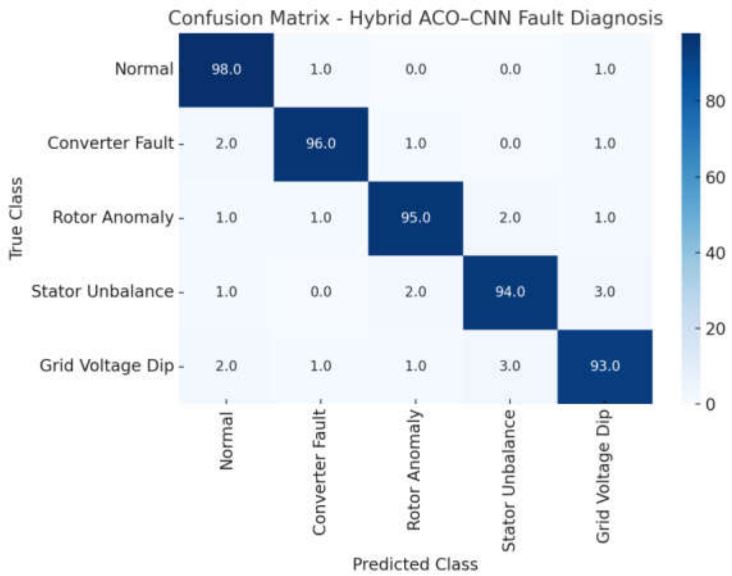

Figure 3 Confusion matrix

ACO preprocessing has been integrated with CNN extracted discriminative features. It enhanced resilience in the inaudible and overlapping failure situations. There was a substantial decrease in false positives. It was vital in the wind farm operation, whereby false alarms led to unnecessary expensive downtimes. Although there were slight overlaps, the framework identified important faults with high confidence [25]. The ACO stage discarded unnecessary and noisy characteristics enabling CNN to generalize. Hybrid ACO CNN had an average accuracy of 95.8%. Table 4 demonstrates the accuracy of the fault diagnosis by the class.

Table 4. Fault Diagnosis Accuracy by Class

Fault Type	Accuracy (%)
Normal Operation	98.0
Converter Fault	96.5
Rotor Anomaly	95.7
Stator Unbalance	94.9
Grid Voltage Dip	93.8

Table 4 showed the accuracy of a system in fault diagnosis of various faults. In the normal operation, the highest accuracy was recorded at 98.0 and this indicates that the system was consistent in deciding when the equipment is in good working conditions. The accuracy was always high in the case of fault conditions. The detection rate of converter faults was 96.5 percent and then there was the detection of rotor anomaly at 95.7 percent. Stator unbalance had a slightly less accuracy of 94.9, whereas grid voltage dip had the lowest accuracy of 93.8. There were some variations that were experienced; however, overall performance was good in all classes, which implies that there was good fault detection ability. The general overall average classification accuracy of 95.8% was used to denote how reliable the system was in distinguishing normal and faulty states.

3. Discussion

The findings explicitly indicated that ACO, which was combined with CNN classification, enhanced fault diagnosis and performance monitoring of wind turbines using DFIG. Preprocessing was an important part of ACO. It had filtered out redundant and less informative features. Only the most topical information was forwarded to the CNN. This selective optimization made the learning better. The CNN dwelled upon noise instead of the patterns that are sensitive to fault. This will result in a stronger and better monitoring. The framework was also found to have good diagnostic capability in more complex and overlapping fault situations [26]. The old models failed to cope with such situations, and the new one coped with it. There were fewer false alarms. All these advantages validated the fact that hybrid ACO-CNN framework was a stable solution. It guaranteed the reliability of operation, stability and grid requirements in real-life wind energy systems. Conceptual performance curve The conceptual performance curve of training accuracy versus epochs is illustrated in Figure 4. ACO-CNN is faster to converge and it is more accurate. The increasing disparity between the two models proves the efficiency and justifies the applicability of the framework in real time fault diagnosis.

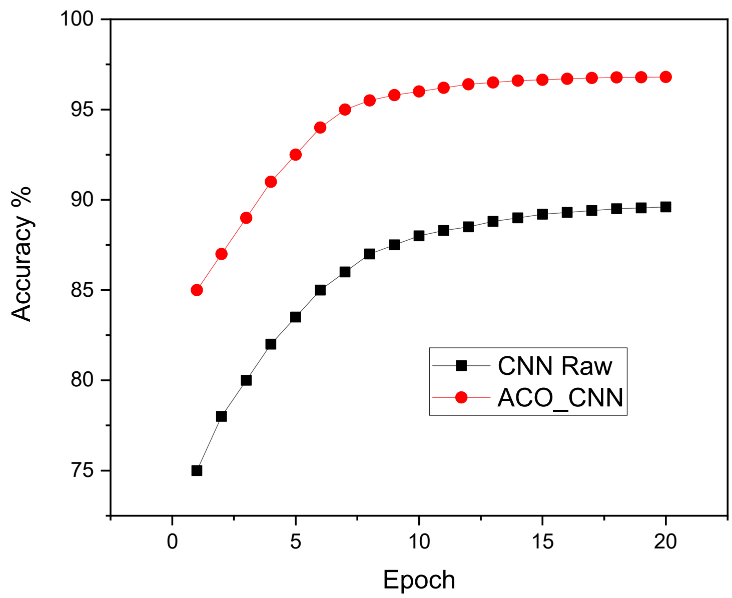

Figure 4: Conceptual Performance Curve (Accuracy vs. Epochs) comparing baseline CNN and proposed ACO–CNN framework.

Conclusions

The work built and confirmed a Hybrid Ant Colony Optimization-Convolutional Neural Network (ACO-CNN) model on the intelligent monitoring and fault diagnosis of DFIG wind turbines. The framework combined ACO based preprocessing and CNN feature learning. Such integration improved the accuracy of diagnoses and trained with less time and became more resistant to noisy. The outcomes of simulations supported the fact that ACO-CNN achieved high performance in comparison with baseline CNN models. The streamlined structure has a total accuracy of 96.8%. It provided dependable classification with normal and faulty operating environments. As well as fault detection, the framework suggested flexibility to variable input signals. This flexibility helps to stabilize and enhance productivity. As the results show, deep learning with the focus on the optimization has the high potential of real-time wind turbine condition tracking and improving the operating quality.

References

1. Loulijat, A., Hilali, A., Makhad, M., Chojaa, H., Ababssi, N., & Mossa, M. A. (2025). Low-voltage ride-through capability of DFIG-based WECS improved by nonlinear backstepping controller synthesized in novel power state model. e-Prime-Advances in Electrical Engineering, Electronics and Energy, 11, 100864.
2. Din, Z., Zhang, J., Xu, Z., Zhang, Y., & Zhao, J. (2021). Low voltage and high voltage ride-through technologies for doubly fed induction generator system: Comprehensive review and future trends. IET Renewable power generation, 15(3), 614-630.
3. Rodríguez, B., Rodríguez, A. J., Sputh, B., Pastorino, R., Naya, M. Á., & González, F. (2022). Energy-based monitoring and correction to enhance the accuracy and stability of explicit co-simulation. Multibody System Dynamics, 55(1), 103-136.
4. Li, X., Sun, G., Kuang, Z., & Han, S. (2022). Nonlinear predictive optimization for deploying space tethered satellite via discrete-time fractional-order sliding mode. IEEE Transactions on Aerospace and Electronic Systems, 58(5), 4517-4526.
5. Danayiyen, Y., Dinçer, K., & Nuhoğlu, Y. (2024). A novel fractional order proportional integral-fractional order proportional derivative controller design based on symbiotic organisms search algorithm for speed control of a direct current motor. Electrica, 24(2), 327-335.
6. Nasri, S., Nowdeh, S. A., Davoudkhani, I. F., Moghaddam, M. J. H., Kalam, A., Shahrokhi, S., & Zand, M. (2021). Maximum Power point tracking of Photovoltaic Renewable Energy System using a New method based on turbulent flow of water-based optimization (TFWO) under Partial shading conditions. In Fundamentals and innovations in solar energy (pp. 285-310). Singapore: Springer Singapore.
7. Dasari, M., Reddy, A. S., & Kumar, M. V. (2022). A comparative analysis of converters performance using various control techniques to minimize the torque ripple in BLDC drive system. Sustainable Computing: Informatics and Systems, 33, 100648.
8. Gorel, G., & Abdi, M. O. (2023). Advanced Pitch Angle Control Based on Genetic Algorithm and Particle Swarm Optimisation on FAST Turbine Systems. Elektronika ir Elektrotechnika, 29(4), 11-18.
9. Huang, X., Mu, F., Liu, Y., Wu, Y., & Sun, H. (2021). Asynchronous gate signal driving method for reducing current imbalance of paralleled IGBT modules caused by driving circuit parameter difference. IEEE Access, 9, 86523-86534.
10. Musarrat, M. N., Fekih, A., & Islam, M. R. (2021). An improved fault ride through scheme and control strategy for DFIG-based wind energy systems. IEEE Transactions on Applied Superconductivity, 31(8), 1-6.
11. Ramalingegowda, C. H., & Rudramoorthy, M. (2022, December). GCSC and TCSC implementation in DFIG based wind farms to mitigate sub synchronous resonance. In 2022

Fourth International Conference on Emerging Research in Electronics, Computer Science and Technology (ICERECT) (pp. 1-7). IEEE.
12. Letaief, F., Hamouda, M., Belaid, M. A., & Al-Haddad, K. (2024). A comprehensive approach to flexible LVRT strategies for inverter-based PPMs enhancing voltage-support, overcurrent protection, and DC-link voltage quality. IEEE Access, 12, 52990-53017.
13. Ntuli, W. K., Kabeya, M., & Moloi, K. (2024). Review of Low Voltage Ride-Through Capabilities in Wind Energy Conversion System. Energies (19961073), 17(21).
14. Khosravi, N., Dowlatabadi, M., Oubelaid, A., & Belkhier, Y. (2025). Optimizing reliability and safety of wind turbine systems through a hybrid control technique for low-voltage ride-through capability. Computers and Electrical Engineering, 123, 110205.
15. Li, Y., Kong, B., Yu, W., & Zhu, X. (2023). An attention-based CNN-LSTM method for effluent wastewater quality prediction. Applied Sciences, 13(12), 7011.
16. Anwar, M. A., Haque, A., Khan, M. Z., & Mateen, S. (2024, July). Enhanced Islanding Detection for Grid-Connected PV Systems: A Machine Learning Approach. In 2024 IEEE 4th International Conference on Sustainable Energy and Future Electric Transportation (SEFET) (pp. 1-6). IEEE.
17. Ahmadzadeh, M., Zahrai, S. M., & Bitaraf, M. (2025). An integrated deep neural network model combining 1D CNN and LSTM for structural health monitoring utilizing multisensor time-series data. Structural Health Monitoring, 24(1), 447-465.
18. Chen, X., Pan, W., Wang, X., & Zhou, Y. (2022). Design of a brushless doubly fed generator with simplified three-phase wound rotor. IEEE Transactions on Industrial Electronics, 70(5), 4427-4439.
19. Ma, K., Chen, Z., Liu, Z., Bak, C. L., & Castillo, M. (2021). Protection collaborative fault control for power electronic-based power plants during unbalanced grid faults. International Journal of Electrical Power & Energy Systems, 130, 107009.
20. Nawrocki, W., Stryjski, R., Kostrzewski, M., Woźniak, W., & Jachowicz, T. (2023). Application of the vibro-acoustic signal to evaluate wear in the spindle bearings of machining centres. In-service diagnostics in the automotive industry. Journal of Manufacturing Processes, 92, 165-178.
21. Ahuja, H., Singh, A., Sharma, S., Sharma, G., & Bokoro, P. N. (2022). Coordinated Control of Wind Energy Conversion System during Unsymmetrical Fault at Grid. Energies, 15(13), 4898.
22. Awadallah, M. A., Makhadmeh, S. N., Al-Betar, M. A., Dalbah, L. M., Al-Redhaei, A., Kouka, S., & Enshassi, O. S. (2025). Multi-objective ant colony optimization. Archives of Computational Methods in Engineering, 32(2), 995-1037.
23. Cong, S., & Zhou, Y. (2023). A review of convolutional neural network architectures and their optimizations. Artificial Intelligence Review, 56(3), 1905-1969.
24. Saeed, S., Asghar, R., Mehmood, F., Saleem, H., Azeem, B., & Ullah, Z. (2022). Evaluating a hybrid circuit topology for fault-ride through in DFIG-based wind turbines. Sensors, 22(23), 9314.
25. Wang, Q., Cui, S., Li, E., Du, J., Li, N., & Sun, J. (2025). Deep Learning-Based Fault Diagnosis via Multisensor-Aware Data for Incipient Inter-Turn Short Circuits (ITSC) in Wind Turbine Generators. Sensors, 25(8), 2599.
26. Liu, X., Zhang, Z., Liu, Y., Yuan, L., Su, M., Zhou, F., ... & Wang, P. (2024). Fault current multi-stages calculation method for DFIG-based wind farms with whole fault process attributes

under asymmetrical grid fault conditions. IEEE Transactions on Sustainable Energy, 15(4), 2361-2379.